N70-11549

ML-1801

INVESTIGATION OF LASER DYNAMICS, MODULATION AND CONTROL BY MEANS OF INTRA-CAVITY TIME VARYING PERTURBATION

under the direction of

S. E. Harris

CASE FILE COPY

Quarterly Status Report

(Report No. 8)

for

NASA Grant NGR-05-020-103

National Aeronautics and Space Administration

Washington, D. C.

for the period

1 August 1969 - 31 October 1969

M. L. Report No. 1801

October 1969

Microwave Laboratory
W. W. Hansen Laboratories of Physics
Stanford University
Stanford, California

STAFF

NASA Grant NGR-05-020-103

for the period

1 August 1969 - 31 October 1969

PRINCIPAL INVESTIGATOR

S. E. Harris

PROFESSORS

A. E. Siegman

R. L. Byer

RESEARCH ASSISTANTS

J. E. Murray

J. Falk

J. F. Young

S. C. Wang

INTRODUCTION

The work under this Grant is generally concerned with the generation, control, and stabilization of optical frequency radiation. In particular, we are concerned with obtaining tunable optical sources by means of nonlinear optical techniques. During this period work was active in the following areas. These were: first, a novel technique to produce long, high-power optical doubled pulses from Q-switched lasers; second, a proposed new method which would allow the output frequency of an optical parametric oscillator to be locked to the absorption of an atomic transition; third, a technique to attain backward oscillation in the far infrared; and fourth, a method to stabilize gas lasers.

During this period the following publications have been submitted for publication and/or have been published:

J. E. Murray and S. E. Harris, "Pulse Lengthening Via Overcoupled Internal Second Harmonic Generation," submitted to J. Appl. Phys.

S. E. Harris, "Tunable Optical Parametric Oscillators," submitted to Proc. IEEE.

1. Pulse Lengthening Via Overcoupled Internal Second Harmonic Generation

(S. E. Harris and J. E. Murray)

We have completed the theoretical analysis of this pulse lengthening technique, and have submitted the results for publication in the J. Appl. Phys. The submitted paper is included as Appendix A.

We are now preparing to demonstrate the effect experimentally using KDP and a ruby laser system.

2. Backward Wave Oscillation

(Joel Falk and S. E. Harris)

The backward wave oscillator as previously proposed involves a three photon interaction which becomes temporally unstable at high pumping levels. During the past quarter backward wave oscillation was attempted in the best quality $LiTaO_3$ available to date. Pumping levels were as high as 200 MW/cm^2 or more than 40 times theoretical threshold. Oscillation was, however, not observed. We attribute the failure of this experiment to the following: (1) The residual loss of the $LiTaO_3$ at the ruby pump wavelength. The $LiTaO_3$ crystals used were yellow in appearance and had losses which varied from 5% to 15% at the ruby wavelength. (2) All crystals used were not nearly optically perfect; i.e., birefringence wander as a function of crystal length was easily observed when the crystals were examined between crossed polarizers.[1] (See Fig. 1)

As a test of quality of the $LiTaO_3$ crystals, attempts were made at observation of stimulated Raman scattering from the 201 cm^{-1} and 600 cm^{-1} A_1 symmetry vibrational modes.[2] Strong backward wave scattering from each mode was readily observed. Attempts at observation of forward wave

[1] J. E. Midwinter, Appl. Phys. Letters 11, 128 (1967).

[2] I. P. Kaminow and W. D. Johnston, Jr., Phys. Rev. 160, 519 (1967).

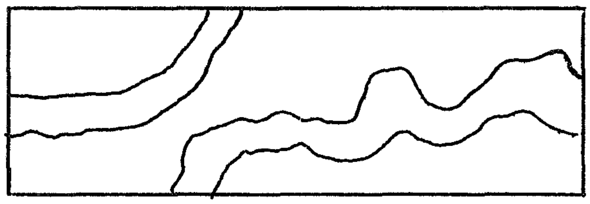

a) Poor Crystal

b) Good Crystal

FIG. 1--Birefringence wander in lithium tantalate as observed between crossed polarizers.

scattering were unsuccessful. We note that the backward wave Raman process does not involve the propagation of a coherent far infrared electromagnetic wave and is hence insensitive to small refractive index changes. On the other hand, forward wave Raman scattering involves a wave of short k vector which is at least partially photon-like and hence crucially dependent on refractive index homogeneity. We attribute the absence of forward wave Raman scattering as further evidence of refractive index variations.

The problems of absorption and refractive index wander in $LiTaO_3$ have led us to suspend oscillation attempts in $LiTaO_3$. During the next quarter attempts at backward oscillation will be made in $LiNbO_3$. $LiNbO_3$ is optically clear at 6943 Å (less than 0.1% absorption per cm) and is available in nearly optically perfect crystals.

The $LiNbO_3$ will be cut with its length at 10^o to the crystal c axis to allow backward wave oscillation to be phase matched at 1.0 mm at 20^oC. At this wavelength $LiNbO_3$ absorption as calculated from measured reflectivity, is less than a few cm^{-1}.[3]

The crystal will be cut so that its length will fall in the crystallographic +c , +a plane such that the contributions to the nonlinear polarizability due to the addition of coefficients d_{42} and d_{22} .[4] It is interesting to note that although in the visible part of the spectrum d_{42} and d_{22} [5] have opposite signs, for far infrared generation they have the same sign. This apparent lack of sign agreement may be understood

[3]J. D. Axe and D. F. O'Kane, Appl. Phys. Letters 9, 58 (1966).

[4]K. F. Hulme, P. H. Davies, and V. M. Cound, J. Phys. C (Solid State Phys.) Ser. 2, 2, 855 (1969).

[5]J. E. Bjorkholm, Appl. Phys. Letters 13, 36 (1968).

by recalling that for visible light generation the nonlinear coefficients are due to nonlinear electronic polarizability while for far infrared generation the nonlinear coefficients are due primarily to nonlinear molecular effects.

The use of a $LiNbO_3$ crystal cut at 10° to the c axis will result in an effective nonlinear coefficient given by

$$d_{eff} = d_{42} \sin \theta + d_{22} \cos \theta \tag{1}$$

where θ is the angle between the crystal c axis and its length. For $LiNbO_3$ $d_{42} = 1.0 \cdot 10^{-21}$ mks, $d_{22} = 0.1 \cdot 10^{-21}$ mks and hence for a 10° cut crystal $d_{eff} = 0.27 \cdot 10^{-21}$ mks. From Eq. (1) we see that the effective nonlinearity is increased as θ is increased toward $\tan^{-1}(d_{42}/d_{22}) = 83^\circ$. Unfortunately the increased nonlinearity that would result from θ near 83° is unusable, inasmuch as phase matching for θ is appreciably greater than 10° and occurs in the lossy region of $LiNbO_3$ where backward wave oscillation is impossible.

We note that cutting of the $LiNbO_3$ at 10° to the c axis introduces walk-off between the extraordinary pump wave normal and its Poynting vector. If care is not taken to make all the parametric beams large, the pump will effectively walk out of the parametric interaction, drastically reducing the interactions's efficiency. It has been shown that for walk-off to be negligible beam size must be greater than $\sqrt{p\ell}$ where p is the walk-off angle and ℓ the crystal length. For a one centimeter 10° cut $LiNbO_3$ crystal this means that beam sizes must be kept greater than 0.19 mm. The restriction of minimum beam size of $\sqrt{2}p\ell$ means, in effect, that for a lossless crystal of $LiNbO_3$ the threshold power required for backward wave oscillation is independent of length and is given by 1.1 MW. This means that any increase in available crystal length manifests itself, not in a decrease in the pump power required, but in an increased minimum pump area and hence a decreased pump power density. Therefore, for backward wave oscillation in a lossless crystal it is advantageous to increase crystal length to a point where required threshold densities will not damage the crystal. Previous experience has indicated that $LiNbO_3$ damages at approximately 150 MW/cm^2. This damage threshold leads to a calculated minimum crystal length of 2.5 cm for avoidance of laser damage at backward wave threshold.

3. Laser Stabilization Studies

(S. C. Wang)

The purpose of this part of the project is to develop methods for absolute frequency stabilization of laser oscillators, particularly for a He-Xe 3.51μ laser. The frequency stabilization can be obtained by two possible methods: one is to stabilize laser oscillation frequency at "enhanced Lamb-dip" of low pressure pure Xe cell inside the laser cavity, and the second is to use saturation of resonance absorption of a proper low pressure gas inside the laser cavity and to lock the oscillation frequency on an "inverted Lamb dip".

During this period, the laser-absorber frequency stabilization method has been investigated. By introducing di-methyl-ether (C_2H_6O) as saturable absorbing gas inside the laser cavity, the "inverted Lamb dip" has been observed and recorded.

The laser cavity is 82.5 cm long with a single isotope xenon laser 20 cm long and an absorbing gas cell 50 cm long filled with C_2H_6O gas. Two separate methods are used to investigate the "inverted Lamb dip" formed due to the saturation of resonance absorption of gas at the laser oscillation line. The first method is the direct measurement of power output versus frequency tuning of cavity, and the second is the detection of the first derivative of output power versus frequency tuning.

The preliminary result of the recorded "inverted Lamb dip" shows that it has a 1 MHz width and an absorption intensity of 4% that of the laser peak value. The investigation is continuing at the present time.

APPENDIX A

PULSE LENGTHENING VIA OVERCOUPLED INTERNAL SECOND HARMONIC GENERATION

by

J. E. Murray and S. E. Harris

PULSE LENGTHENING VIA OVERCOUPLED INTERNAL SECOND HARMONIC GENERATION*

by

J. E. Murray and S. E. Harris

ABSTRACT

This paper discusses the use of internal second harmonic generation as a means of lengthening the pulses of Q-switched lasers. The second harmonic generator acts as both a nonlinear power dependent loss and as an output coupler for the laser. The lengthening arises if the coupling to the second harmonic is greater than that necessary to maximize the peak second harmonic power. It is shown that a pulse lengthening factor of about 100 should be obtainable.

*This work was sponsored by the National Aeronautics and Space Administration, under NASA Grant NGR-05-020-103.

Introduction

In many nonlinear applications, pulses which are somewhat longer than may be obtained from normal Q-switched lasers are desirable. Such pulses would allow interactions to reach steady state and also reduce the possibility of various types of optical damage. Several authors have described techniques which make use of a nonlinearly increasing loss to achieve this pulse lengthening.[1-8] Such techniques have employed stimulated Rayleigh, Raman, and Brillouin scattering,[2,3] two photon absorption,[4-7] and nonlinear free carrier generation[4,6] as the means of obtaining the nonlinear loss. In this paper we describe the use of second harmonic generation as the internal loss mechanism.[4] In applications where the useful output is the second harmonic of the pumping laser, this approach is particularly advantageous because the pulse lengthening is achieved at no expense in output energy.

In the technique proposed here, the nonlinear doubling crystal is placed inside the laser cavity where it acts as both the output coupling for the laser and as the nonlinear loss. As the laser power builds up, the loss resulting from second harmonic generation increases as the square of the fundamental power; peak power is reached when this loss has increased to where it is equal to the single pass gain. Once this gain equals loss point is reached, the laser power may no longer increase, and the remaining population inversion is used in lengthening the pulse. If the coupling to the second harmonic is substantially greater than that necessary to optimumly couple, i.e. to produce the maximum peak power at the second harmonic wavelength, then the majority of the inversion will be used to lengthen the pulse. For such output couplings there is a direct trade off between pulse amplitude and length, and the energy of the second harmonic pulse remains constant as a function of second harmonic coupling.

Theory

The rate equations[9] for a laser system with an additional term in the photon density equation representing the loss to second harmonic generation are

$$dN/dt = W - (\sigma c/LA)uN - N/\tau_{tot} \quad (1)$$

$$du/dt = - u/\tau_c + (\sigma c/LA)N(u + 1) - Ku^2 \quad (2)$$

where

N = Population inversion

W = Pumping rate

u = Total number of photons per pertinent cavity mode

τ_c = Photon lifetime

τ_{tot} = Total lifetime of upper state

K = Nonlinear coupling coefficient

L = Optical length of resonator

A = Beam area in laser material

σ = Cross section for the laser line of interest

$= \lambda^2/4\pi^2\epsilon\tau_\ell\Delta\nu$

ϵ = Relative dielectric constant

τ_ℓ = Radiative spontaneous lifetime of upper state

$\Delta\nu$ = Full half-power linewidth

In terms of the second harmonic crystal parameters, K is given by

$$K = h\nu \left(\frac{c}{L}\right)^2 \frac{P_{SH}}{P_F^2}$$

$$= \frac{8\pi h}{w^2} (\eta\nu)^3 (d\ell)^2 \left(\frac{c}{L}\right)^2$$

where

P_F = Internal fundamental power

P_{SH} = Generated second harmonic power

w = Fundamental beam radius in second harmonic crystal

η = 377/refractive index of nonlinear crystal at second harmonic

ν = Fundamental laser frequency in Hertz

ℓ = Length of nonlinear crystal

d = Nonlinear coefficient

and where near field focusing has been assumed.[10]

For Q-switched operation,[11,12] the pumping term and the spontaneous emission terms can be neglected and equations (1) and (2) may be normalized to yield

$$dn/dT = -\phi n \tag{3}$$

$$d\phi/dT = \phi(n - 1) - \beta\phi^2 \tag{4}$$

where

$n = N/N_{th} = (\sigma c/LA)\tau_c N$

$\phi = (\sigma c/LA)\tau_c u$

$T = t/\tau_c$

$\beta = (LA/\sigma c)K$

We will define β as the normalized coupling parameter; it can also be written

$$\beta = \left(\frac{c}{L}\right) \times \left(\frac{\text{Second harmonic conversion efficiency per fundamental power}}{\text{Single pass gain per stored energy in inversion.}}\right)$$

where the second harmonic conversion efficiency is defined as P_{SH}/P_F.

Results

Figures 1 through 5 show normalized second harmonic pulse length, peak second harmonic power, normalized second harmonic energy, fundamental pulse width, and peak fundamental power as a function of the normalized initial inversion n and the normalized coupling parameter β. The relations between the actual parameters and the normalized ones are

$$P_{SH} = (h\nu LA/\sigma c \tau_c^2)\beta\phi^2$$

$$P_{Fund} = (h\nu A/\sigma\tau_c)\phi$$

$$E_{SH} = (h\nu LA/\sigma c\tau_c)\varepsilon_{SH}$$

From Figs. 1 and 4 it is seen that until β is greater than 1, very little pulse lengthening is obtained. Note that Fig. 3 confirms that once the coupling exceeds approximately 10, the energy in the second harmonic pulse remains constant, giving a direct trade-off between peak amplitude and pulse length. Figure 6 shows the computer-generated second harmonic pulse shapes for $n_0 = 2.0$ and five different values of β. Figure 7 shows the value of β which maximizes the second harmonic peak power for a given value of initial inversion.

Unlike the cw case,[13,14] this optimum coupling for a Q-switched laser is a function of the initial inversion. Figure 8 shows the peak second harmonic power that may be obtained from such an optimumly coupled laser.

The range of validity of these solutions is limited to the region where the generated second harmonic power is nearly proportional to the square of the fundamental power. For an exact large signal solution, it would be necessary to replace the $\beta\phi^2$ term in equation (4) by

$$(c\tau_c/L)\phi \tanh^2 \left[(\beta L/\tau_c c)\phi \right]^{1/2} .$$

However, if this is done, the equations do not normalize to a single parameter. If we require that the argument of the hyperbolic tangent function be less than 0.45, the error introduced to the differential equations by the small amplitude approximation is less than 12%. This condition can be written

$$(\beta L/\tau_c c)\phi = \beta\phi\alpha < 0.2 ,$$

where α is all single pass cavity losses except that due to second harmonic generation. Using this relation and Fig. 5, the regions of validity according to the above criteria can be obtained for any value of cavity loss, α .

Parameters for Some Common Nonlinear Crystals and Lasers

Table I gives cross sections and normalized coupling parameters for a few of the common second harmonic crystals and laser lines. For 90° phase matchable crystals such as $LiNbO_3$ and $Ba_2NaNb_4O_{15}$ the fundamental beam radius used in determining β was taken to be that which would confocally focus a 1/2 cm crystal at the fundamental wavelength. For crystals such as KDP, $LiIO_3$, and α - HiO_3 which exhibit walk-off, the fundamental beam size was chosen according to the criteria $w_0 = \sqrt{2}\ \rho\ell$ where ρ is the walk-off angle in radians and ℓ the crystal length. This criteria is somewhat conservative in terms of the total second harmonic power which may be obtained from the laser, but it ensures a good Gaussian mode.[10] We have assumed a beam radius of 0.75 mm in the laser material and a cavity length of 60 cm; and all values of β are quoted without regard to damage thresholds.

ACKNOWLEDGEMENTS

We are happy to acknowledge the help of R. W. Wallace in calculating the numerical data of Table I and Figs. 7 and 8, and for many helpful discussions.

REFERENCES

1. C. H. Thomas and E. V. Price, J. Quant. Electr. 2, 617 (1966).
2. R. H. Pantell and J. Warszawski, Appl. Phys. Letters 11, 213 (1967).
3. R. Callen, R. H. Pantell, and J. Warszawski, unpublished.
4. J. Schwartz, C. S. Naiman, and R. K. Chang, Appl. Phys. Letters 11, 242 (1967).
5. V. A. Aleshkevich, V. V. Aresn'ev, V. S. Dneprovskii, D. N. Klyshko, and L. A. Sysoev, JETP Letters 9, 123 (1969).
6. A. Hordvik, IEEE Conference on Laser Engineering and Applicaitons, Washington, D. C., 1969, Session 3.1.
7. L. M. Lisitsyn, JETP Letters 9, 165 (1969).
8. I. F. Balashov, V. A. Berenberg, and B. A. Ermakov, Soviet Phys.—Tech. Phys. 13, 699 (1968).
9. R. Dunsmuir, J. Electr. and Contr. 10, 456 (1961); and D. G. Carlson, J. Appl. Phys. 39, 4369 (1968).
10. G. D. Boyd and D. A. Kleinman, J. Appl. Phys. 39, 3597 (1968).
11. F. J. McClung, R. W. Hellwarth, IEEE 51, 46 (1963).
12. W. G. Wagner, B. A. Lengyel, J. Appl. Phys. 34, 2040 (1963).
13. R. Polloni and O. Svelto, J. Quant. Electr. 4, 528 (1968).
14. J. E. Geusic, H. J. Levinstein, S. Singh, R. G. Smith, L. G. Van Uitert Appl. Phys. Letters 12, 306 (1968).

TABLE I

Transition cross sections and normalized coupling parameters for a few laser lines and second harmonic crystals

Laser System	$\sigma(cm^2)$	β				
		KDP[e,f]	α-HIO_3[e,g]	$LiIO_3$[h,i]	$LiNbO_3$[j,k]	$Ba_2NaNb_5O_{15}$[ℓ,m]
Nd^{3+}:YAG 0.946 μ	6.3×10^{-20} [a,b]	8.2	60	3.0×10^2	8.3×10^4	7.2×10^5
Nd^{3+}:YAG 1.064 μ	8.8×10^{-19} [b]	0.47	3.7	14	3.8×10^3	3.3×10^4
Nd^{3+}:YAG 1.318 μ	2.9×10^{-19} [c,b]	0.89	4.1	21	4.9×10^3	4.3×10^4
Ruby 0.694 μ	2.0×10^{-20} [d]	84	--	4.7×10^3	--	--

TABLE I

REFERENCES

a. S. E. Harris and R. W. Wallace, IEEE Conference on Laser Engineering and Application, Washington, D. C., 1969.

b. T. Kushida, H. M. Marcos, and J. E. Geusic, Phys. Rev. 167, 289 (1968).

c. U. Deserno, D. Ross, and G. Zeidler, Phys. Letters 28A, 422 (1968).

d. D. F. Nelson and M. D. Struge, Phys. Rev. 137A, 117 (1965).

e. J. E. Bjorkholm, J. Quant, Electr. QE-4, 970 (1968); and errata, J. Quant. Electr. QE-5. 260 (1969).

f. F. Zernike, Jr., J.O.S.A. 54, 1215 (1964); and errata, J.O.S.A. 55, 210 (1965).

g. S. K. Kurtz, T. T. Perry, and J. G. Bergman, Jr., Appl. Phys. Letters 12, 186 (1968).

h. G. Nath and S. Haussukl, Appl. Phys. Letters 14, 154 (1969).

i. G. Nath and S. Haussukl, Phys. Letters 29A, 91 (1969).

j. R. L. Byer and S. E. Harris, Phys. Rev. 168, 1064 (1968).

k. G. D. Boyd, R. C. Miller, K. Nassau, W. L. Bond and A. Savage, Appl. Phys. Letters 11, 234 (1964).

ℓ. J. E. Geusic, H. J. Levinstein, J. J. Rubin, S. Singh, and L. G. Van Uitert, Appl. Phys. Letters 11, 269 (1967); and errata, Appl Phys. Letters 12, 224 (1968).

m. S. Singh, unpublished (1968).

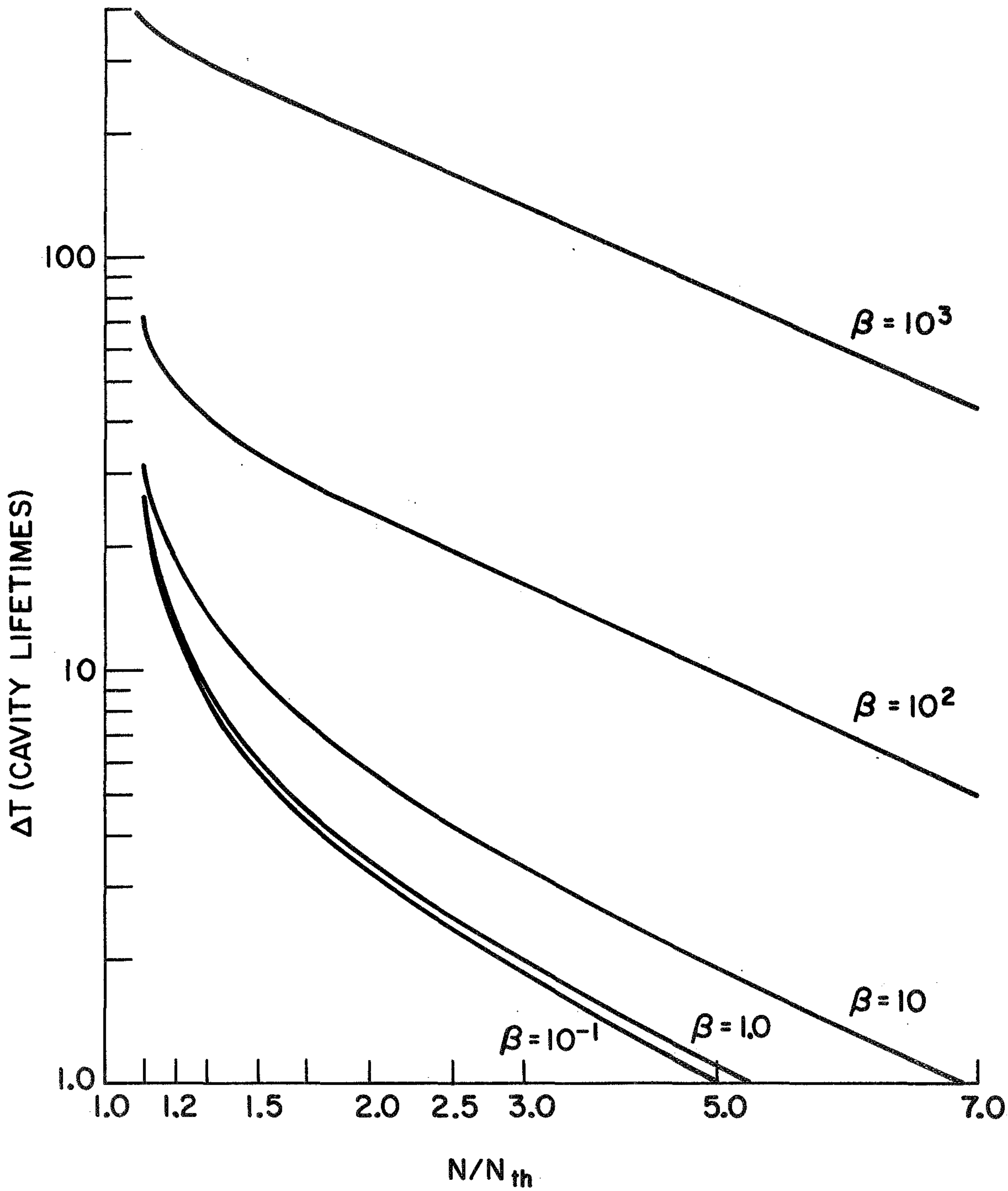

FIG. 1--Second harmonic pulse length versus initial inversion.
ΔT = full width at half amplitude.

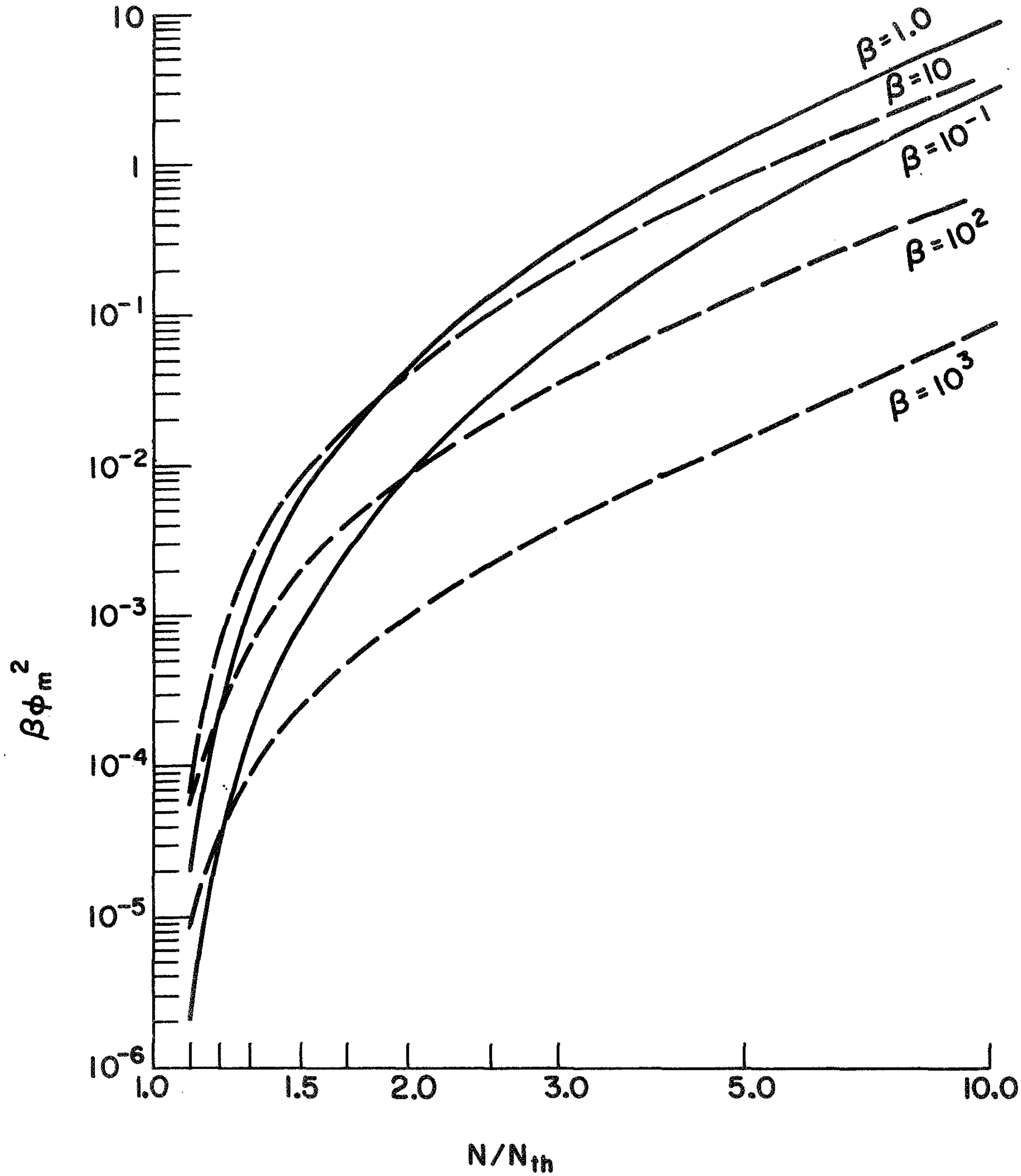

FIG. 2--Peak second harmonic power versus initial inversion. This gives the total second harmonic power generated and doesn't account for the fact that it is typically generated in both directions.

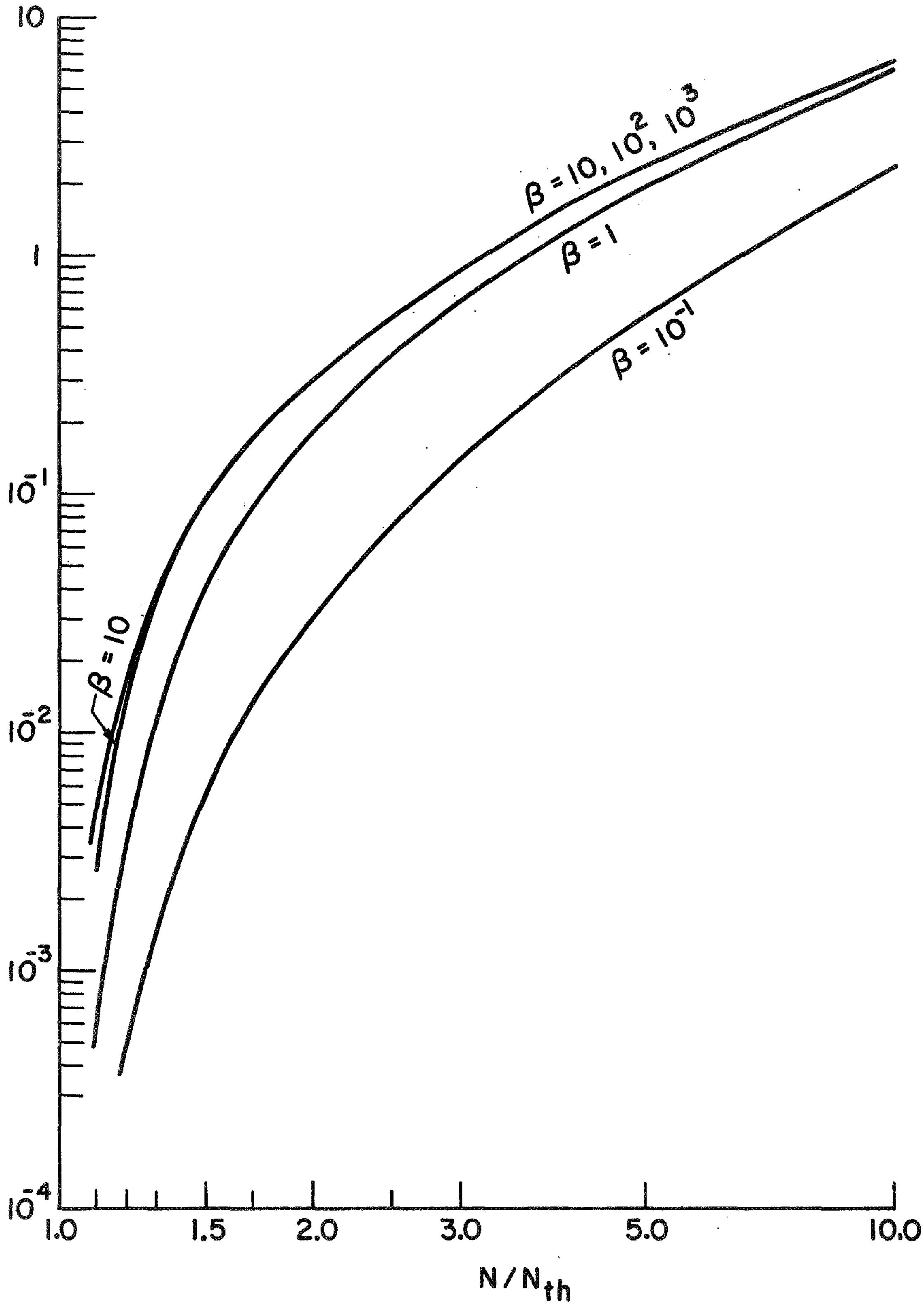

FIG. 3--Normalized second harmonic energy versus initial inversion.

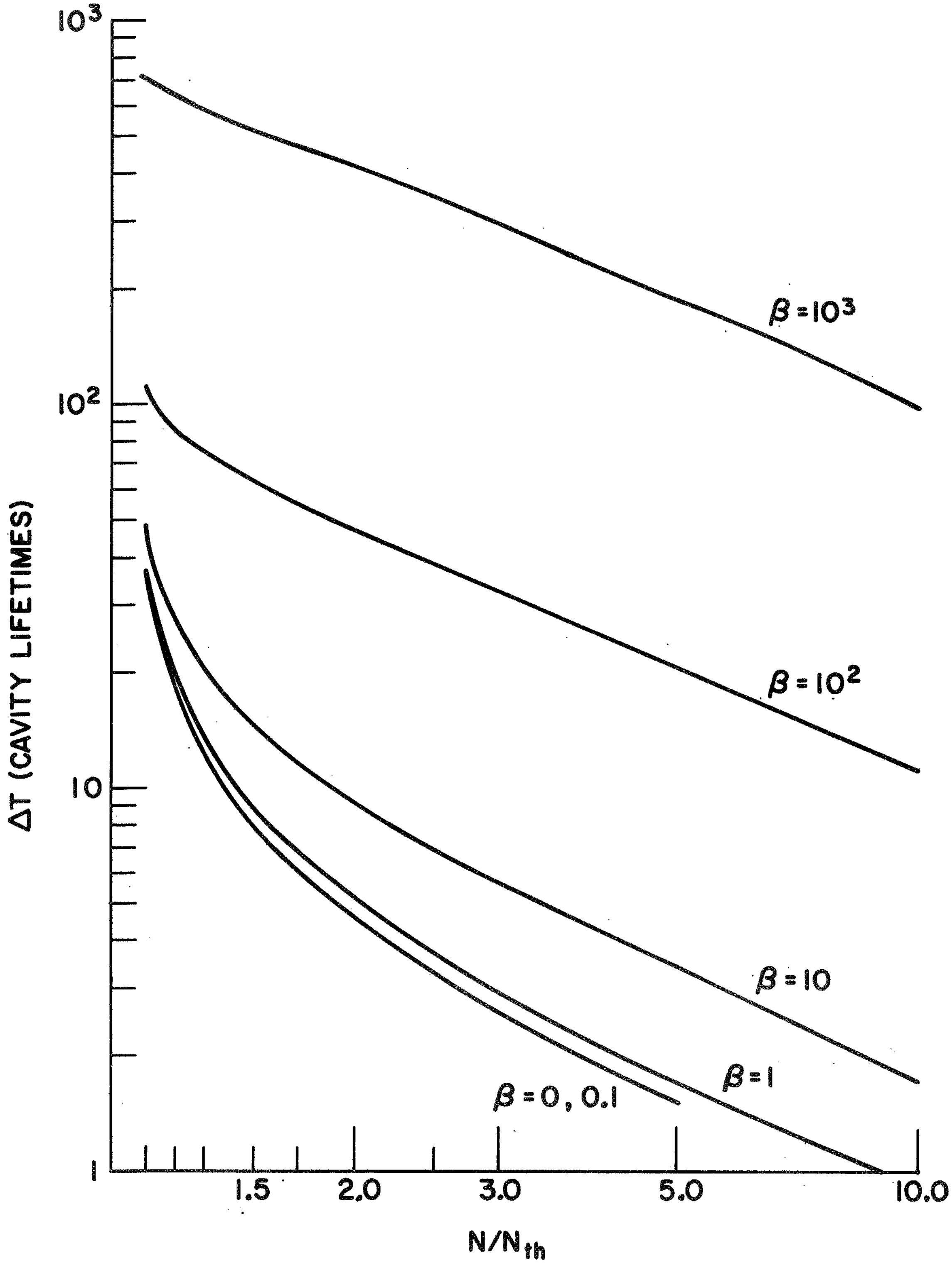

FIG. 4--Fundamental pulse length versus initial inversion.
ΔT = full width at half amplitude.

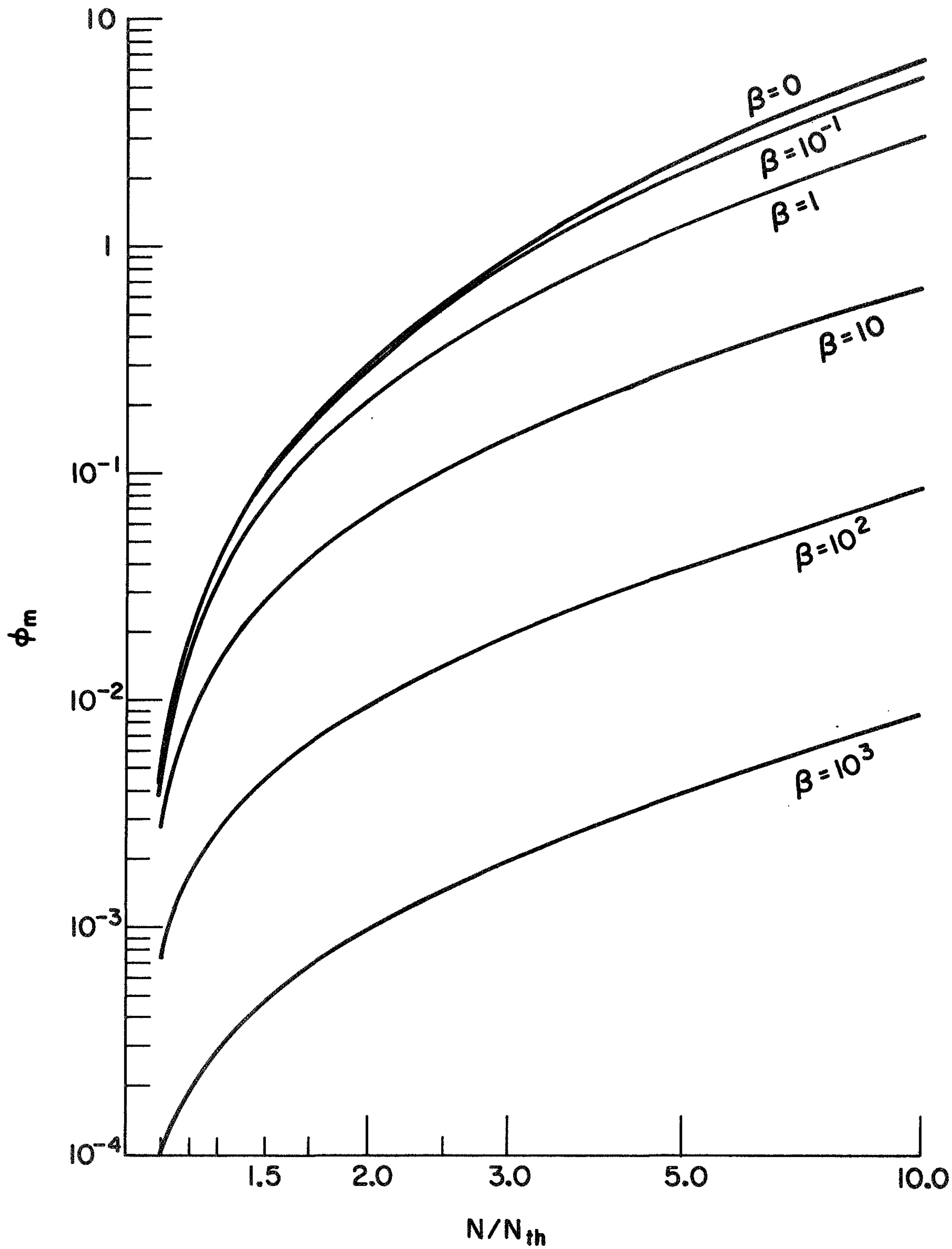

FIG. 5--Peak fundamental power internal to the laser cavity versus initial inversion.

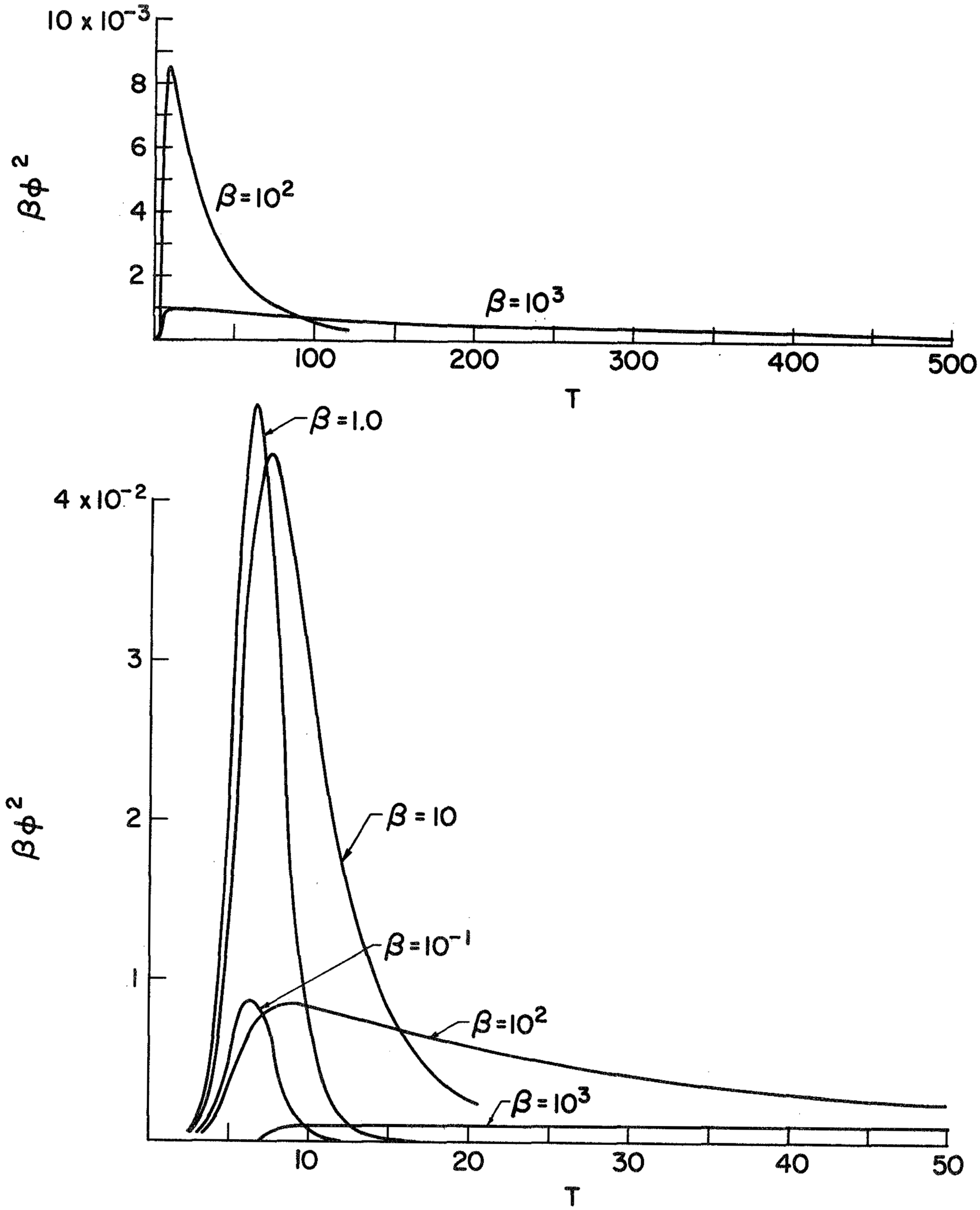

FIG. 6--Computer generated waveforms for five values of the normalized coupling parameter, β , and an initial inversion of 2.0. The upper figure shows the waveforms for $\beta = 10^2$ and 10^3 with an expanded time scale.

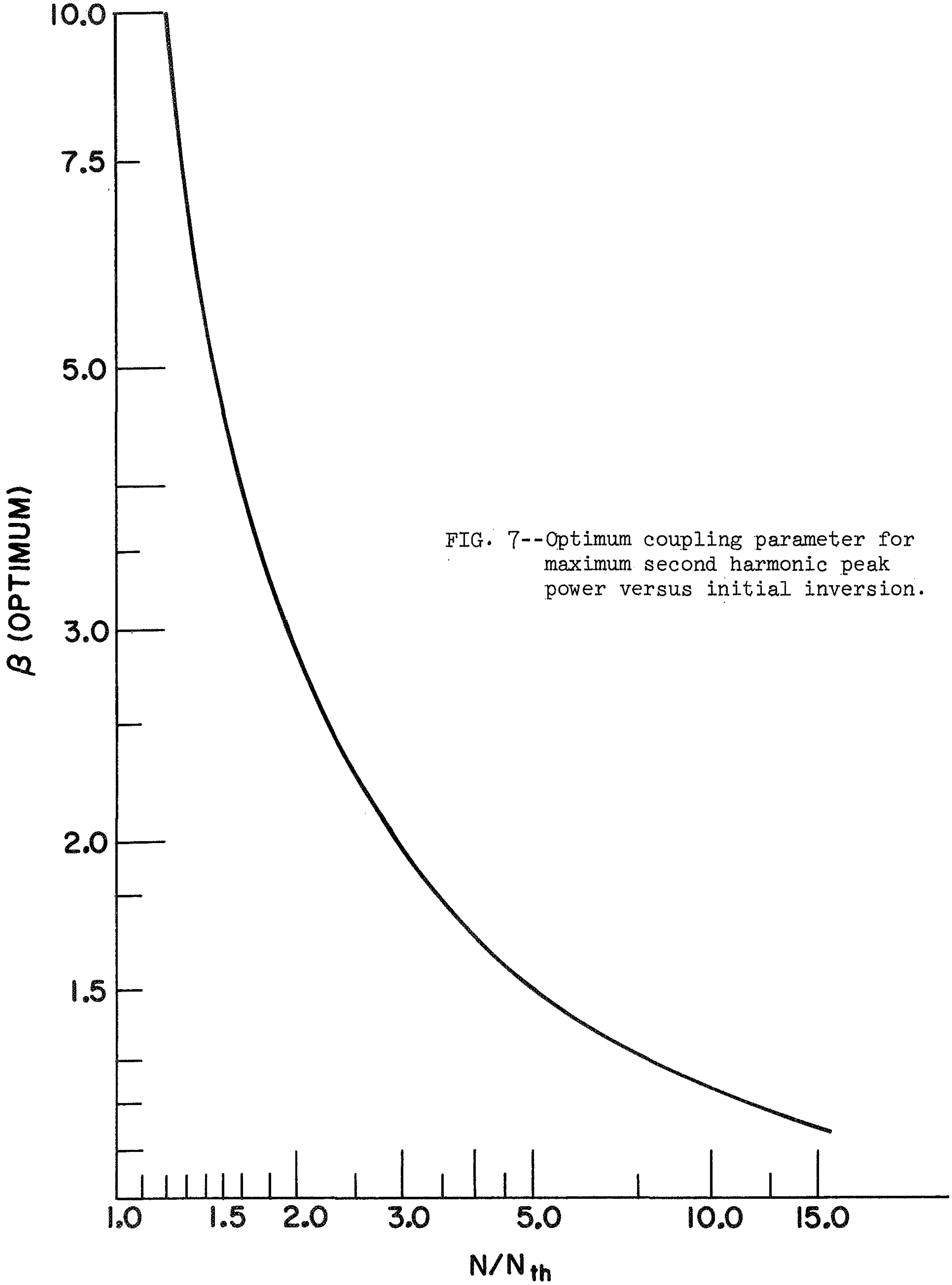

FIG. 7--Optimum coupling parameter for maximum second harmonic peak power versus initial inversion.

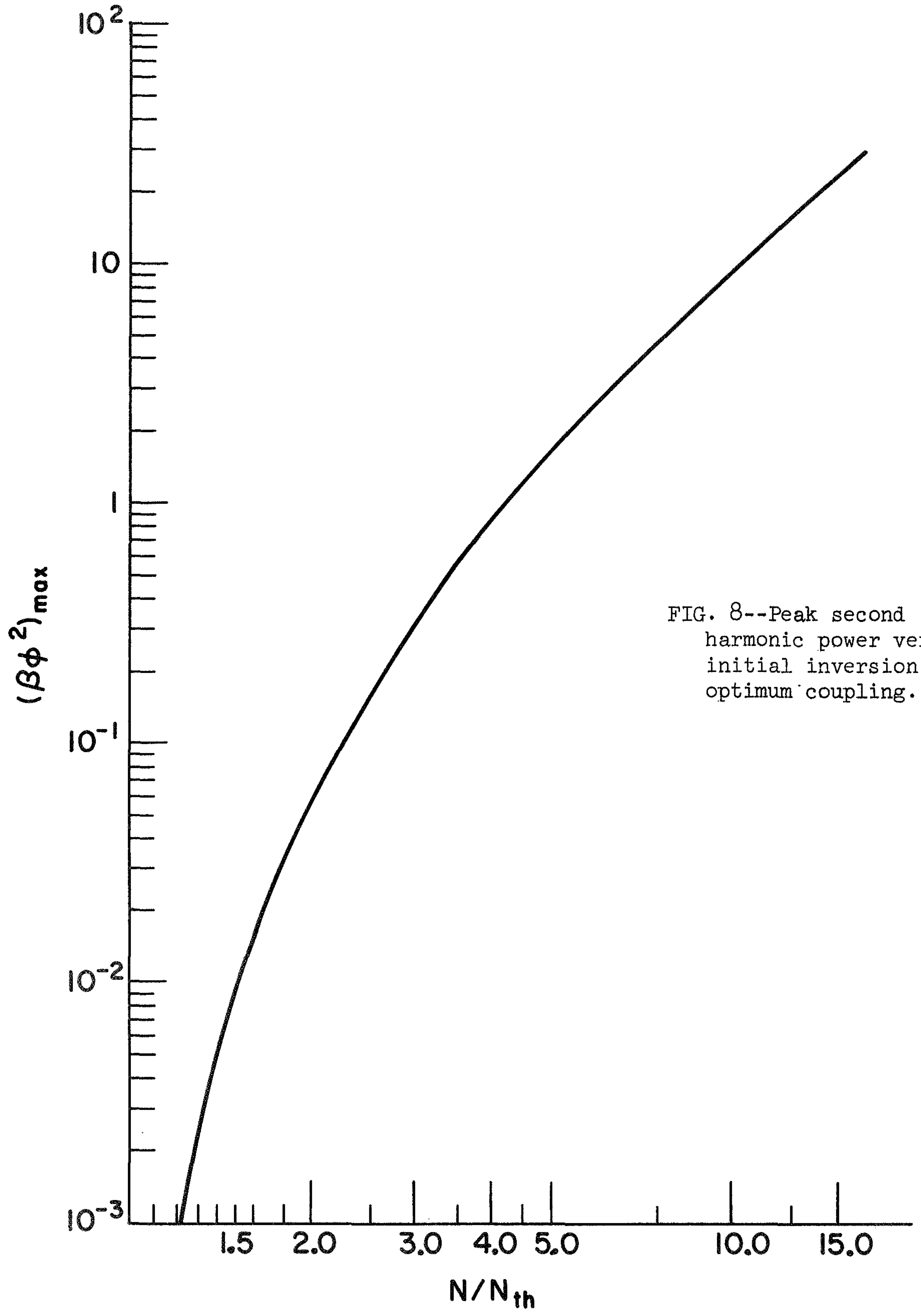

FIG. 8--Peak second harmonic power versus initial inversion for optimum coupling.